Appl. Phys. B (2007)
DOI: 10.1007/s00340-006-2560-z

**Applied Physics B**
**Lasers and Optics**



V. KOSKINEN[1,✉]
J. FONSEN[1]
K. ROTH[1,2]
J. KAUPPINEN[1]

# Cantilever enhanced photoacoustic detection of carbon dioxide using a tunable diode laser source

[1] Department of Physics, University of Turku, 20014 Turku, Finland
[2] Gasera Ltd.*, Tykistökatu 4, 20520 Turku, Finland

**Received: 29 August 2006 / Revised version: 29 November 2006**


**ABSTRACT** Recently introduced cantilever enhanced photoacoustic sensing has been applied to the tunable diode laser-based trace gas detection. The pressure variations due to the photoacoustic signal are detected with a miniature silicon cantilever, whose displacement is measured with a compact Michelson type laser interferometer. The system has been used to detect carbon dioxide ($CO_2$) at 1572 nm with a distributed feedback diode laser. With a new photoacoustic cell, that was optimized for the laser sources, a normalized noise equivalent sensitivity of $1.7 \times 10^{-10}$ cm$^{-1}$W/$\sqrt{\text{Hz}}$ at atmospheric pressure was realized. The result obtained in the non-resonant operation mode is at least 10 times better than in previous reports. The future improvements of the technique are also discussed.

**PACS** 07.07.Df; 42.55.Px; 82.80.Kq

## 1 Introduction

The requirement for highly sensitive trace gas detection is widely recognized in many fields of applications [1, 2]. Therefore a number of both spectroscopic and non-spectroscopic techniques are used. In many spectroscopic techniques the absorption of the infrared radiation is measured indirectly by comparing the transmitted beam with the incident beam. Since the responses of the IR detectors are already very close to their theoretical limits, the sensitivity of these methods depends mainly on the absorption path length and the radiation power. Photoacoustic (PA) detection, in contrast, offers compact sensors, whose sensitivity is limited by the pressure sensor, i.e., by the capacitive microphone.

Photoacoustic spectroscopy (PAS) is a sensitive and selective method for trace gas analysis, especially if powerful laser sources are used to generate the signal. In PAS the modulated photon beam interacts with the sample material and the absorbed energy is transformed into heat. This results in pressure waves, which are conventionally detected with a microphone. The measured signal is directly proportional to the absorbed energy, and thus PAS is a zero background technique. The best sensitivities to date (NNEA – normalized noise equivalent absorption coefficient [3]) are obtained by exploiting the acoustical resonances of the PA cell, and are typically of the order of $10^{-8}$–$10^{-9}$ cm$^{-1}$W/$\sqrt{\text{Hz}}$ [4–6].

Recently, novel approaches are presented to replace the capacitive microphones in a PA setup. Kosterev et al. [7] used a small quartz tuning fork as a resonant element, by which the acoustical signal was detected. So far, the best result with this method is $5.4 \times 10^{-9}$ cm$^{-1}$W/$\sqrt{\text{Hz}}$ [3]. We have presented another method, where the microphone was replaced with a micromachined silicon cantilever [8]. The displacement of the cantilever due to pressure waves is measured via a compact Michelson-type laser interferometer. Measurements with a broadband IR source and an optical filter suggested a sub-ppb detection limit for methane gas.

We have also demonstrated the potential of the cantilever detection with a tunable diode laser (TDL) source. Even though we used a PA cell designed for broadband sources this resulted in an NNEA of $4.6 \times 10^{-9}$ cm$^{-1}$W/$\sqrt{\text{Hz}}$ when detecting carbon dioxide at 1572 nm [9, 10]. In this study we have repeated those measurements with a cell whose diameter is reduced from 10 to 3 mm; this modification increases the average intensity entering the cell by a factor of 11. The cantilever was also replaced with a new one that allowed the use of lower modulation frequencies. By means of these improvements we managed to reduce the NNEA to $1.7 \times 10^{-10}$ cm$^{-1}$W/$\sqrt{\text{Hz}}$.

## 2 Experimental

### 2.1 *Measurement setup*

The experimental setup is shown in Fig. 1. The diode laser current and temperature drivers were used to tune the wavelength of the distributed feedback (DFB) telecom diode laser (Furukawa Electric FOL 15DCWD-A81-19060) to the desired absorption line of carbon dioxide ($CO_2$) at 1572.018 nm. This fairly weak rotational line R(18) in the $[00^00]_{\text{I}} \rightarrow [30^01]_{\text{II}}$ vibrational band was selected for measurement by the laser availability. The selected absorption line and the Voigt profile simulation based on HITRAN 2004 [11] database at 296 K

✉ Fax: +358-2-3335070, E-mail: vesa.koskinen@utu.fi
*http://www.gasera.fi

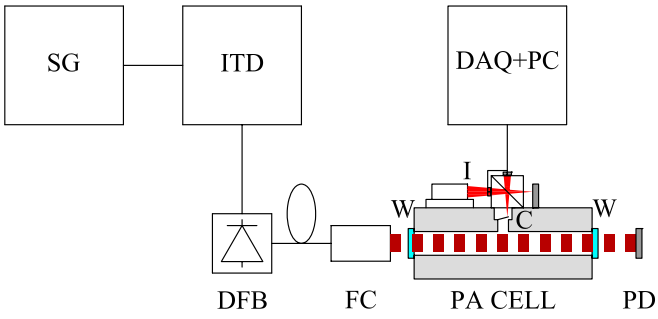


**FIGURE 1** Setup for the measurements: SG – signal generator, ITD – current and temperature driver, DFB – diode laser, FC – fiber collimator, W – $CaF_2$ windows, I – interferometer, C – cantilever and PD – power detector

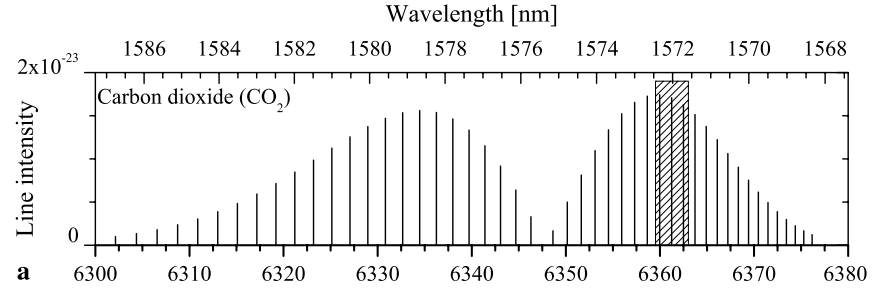


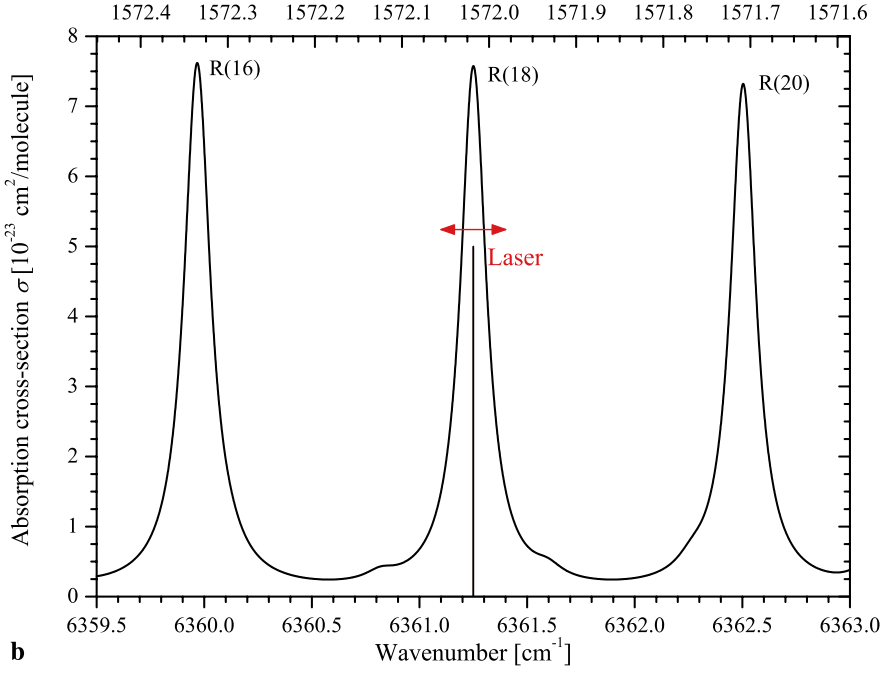


**FIGURE 2** HITRAN 2004 based simulation of the investigated $CO_2$ lines by assuming a Voigt profile at 296 K temperature and atmospheric pressure

temperature and atmospheric pressure are shown in Fig. 2.

During the measurements the power of the laser was held at 30 mW, and the wavelength modulation at half of the detection frequency was performed by modulating the laser current. The beam was collimated with a fiber collimator before entering the cylindrical PA cell, which was sealed with calcium fluoride windows at both ends. All the measurements were made at constant temperature at atmospherical pressure.

### 2.2 *Photoacoustic detector*

The PA signals were measured using a detector provided by Gasera.

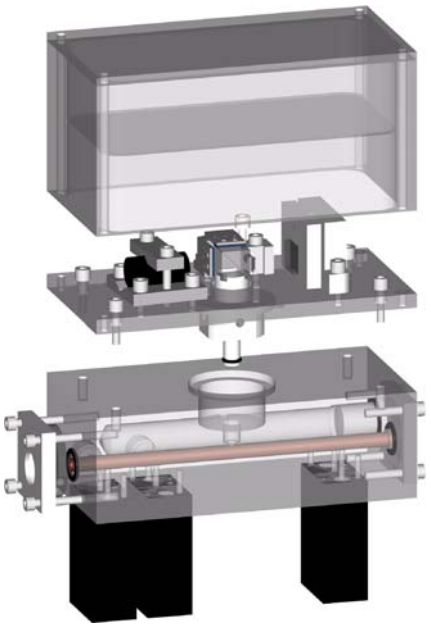

**FIGURE 3** An exploded view of the photoacoustic detector for laser sources provided by Gasera

The detector, shown in Fig. 3, consists of three modules. The lowest part is the base module, which contains the PA cell, the larger expansion cell and the gas connections. The cells are connected to each other through a narrow gap between the cantilever and its frames. The middle part is the interferometer module with the cantilever and the third part is the top case with electronics and connections.

The displacement of the cantilever was monitored via a compact interferometer, whose arms were set to equal length. The laser beam ($\lambda = 670$ nm) was focused very close to the free end of the cantilever and the fringe pattern was adjusted in order to obtain four orthogonal signals from the photodiodes. Digital signal processing was used to calculate the signal proportional to the cantilever displacement and further on its FFT spectrum.

### 2.3 *Frequency response*

The measured frequency response of the sensor and the noise spectrum (measured with the laser turned off) are presented in Fig. 4. The response curve shows that the signal increases as the modulation frequency decreases except frequencies below 5 Hz, where the leakage through the gap of the cantilever acts as a high pass filter.

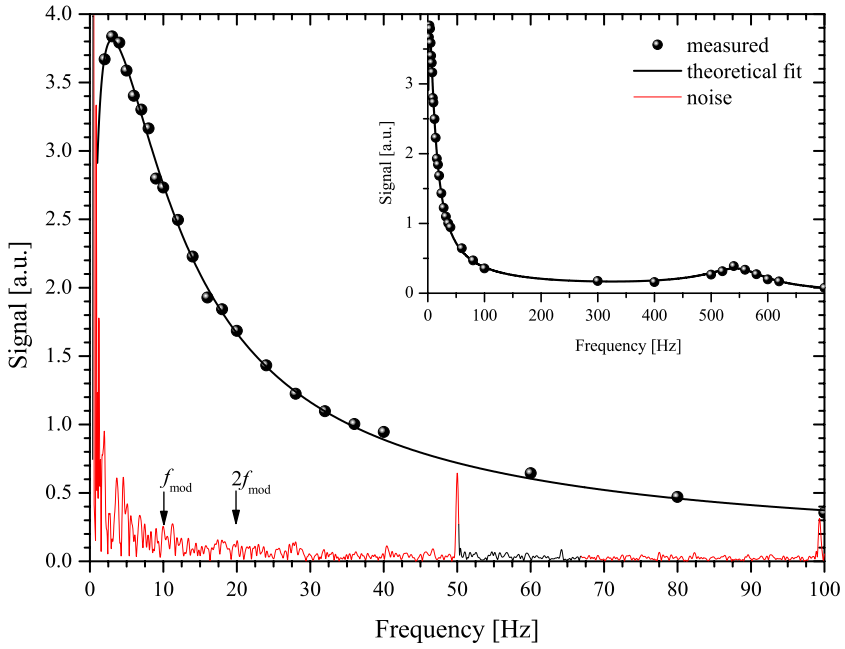


**FIGURE 4** The frequency response of the cantilever inside the PA cell and the noise spectrum

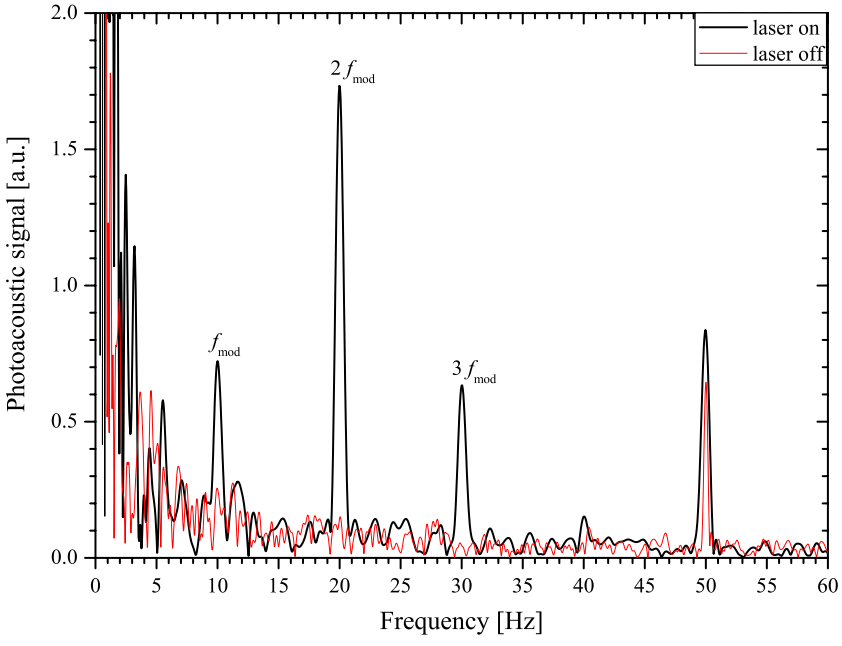


**FIGURE 5** The FFT spectrum of the photoacoustic signal due to 97 ppm of $CO_2$ in argon at atmospheric pressure with a 2.6 s measurement time. The noise spectrum is obtained with the laser turned off

The inset shows a broad resonance peak of the cantilever near 550 Hz but there is no advantage in exploiting it because also the noise follows the frequency response curve. Actually, the signal to noise ratio is constant from 5 Hz up to 600 Hz. With our next setup we will be able to reduce the noise level at low frequencies and therefore the modulation frequency was already chosen as low as possible ($f_{mod} = 10$ Hz). It should be notified that no acoustical resonances of the PA cell were used which enables the use of the detector for example in FTIR applications.

### 2.4 *Detection limit*

In this study, we concentrated on determining the sensitivity of the detector, since the linearity of the measurements was proven previously [12, 13]. The gas chambers were first evacuated with a vacuum pump and then filled to atmospheric pressure with a certified 97.1 ppm ±0.1% of $CO_2$/Ar gas mixture. A FFT spectrum of one of the measured signals is shown in Fig. 5 indicating a peak due to the PA signal at 20 Hz, as expected. The peak at 50 Hz is the interference of the electrical network but the notable peaks at 10 and 30 Hz suggest that the modulation of the laser wavelength was not fully symmetrical. The laser was turned off to measure the noise spectrum whose rms value between 12.5 and 27.5 Hz was used as the noise level. With the signal at 20 Hz, this corresponds to the detection limit of 1.9 ppm and the minimum detectable absorption coefficient ($\alpha_{min}$) of $3.6 \times 10^{-9}$ cm$^{-1}$. This can be normalized with the laser power and the measurement time to determine NNEA of $1.7 \times 10^{-10}$ cm$^{-1}$W/$\sqrt{\text{Hz}}$. At the end of the measurements, the laser was tuned slightly away from the absorption line. The absence of the PA signal at modulation frequency or its multiples proved that there were not any detectable background effects in spectra that were used in the determination of the sensitivity. The summary of the measurement parameters and of the achieved results is presented in Table 1.

## 3 Conclusions

We have used a photoacoustic cell designed for laser sources to improve the sensitivity of the cantilever enhanced photoacoustic detection of trace gases. To our best knowledge, the realized NNEA of $1.7 \times 10^{-10}$ cm$^{-1}$W/$\sqrt{\text{Hz}}$ is the best ever reported in TDLPAS. However, the achieved detection limit for $CO_2$ was relatively high (0.3 ppm with a 100 s measurement time). This is mainly explained by the weakness of the investigated absorption line and the relatively low laser power. In the case of strongly absorbing gases (e.g. methane and ammonia have two orders of magnitude stronger absorption lines in the near IR region than the measured $CO_2$ line) the detection limits can be estimated to be in the ppb level and the sub-ppb level is easily reachable by using fiber amplifiers to increase the laser output power. The operation in non-resonant mode enables the detector to be also used in FTIR measurements.

| Parameter | Value |
|---|---|
| Center wavenumber, $\nu_0$ [cm$^{-1}$] | 6361.250 |
| Center wavelength, $\lambda_0$ [nm] | 1572.018 |
| Line intensity, $S$ [cm$^{-1}$/(molec.cm$^{-2}$)] | $1.708 \times 10^{-23}$ |
| Absorption cross section, $\sigma$ [cm$^2$/molec.] | $7.5 \times 10^{-23}$ |
| Optical power, $P$ [mW] | 30 |
| Measurement time, $t$ [s] | 2.6 |
| Absorption path length, $l$ [cm] | 11.5 |
| $CO_2$ detectivity [ppm] | 1.9 |
| Minimum detectable absorption coefficient $\alpha_{\min}$ [cm$^{-1}$] | $3.6 \times 10^{-9}$ |
| Min. detectable optical density, $\alpha_{\min} l$ | $4.1 \times 10^{-8}$ |
| NNEA [cm$^{-1}$W/$\sqrt{\text{Hz}}$] | $1.7 \times 10^{-10}$ |

**TABLE 1** The summary of the measurement parameters and the results of the work

In future, the measurement setup can be further improved by optimizing the total pressure in the PA cell together with the depth and the symmetricity of the laser wavelength modulation. The absorption path length can be easily doubled by replacing the other window with a mirror and the reduction of the noise at low frequencies will remarkably enhance the performance of the system.

**ACKNOWLEDGEMENTS** The authors wish to thank Rolf Hernberg and his coworkers at Tampere University of Technology for providing the diode laser source.

## REFERENCES

1 K.H. Michaelian, *Photoacoustic Infrared Spectroscopy* (Chemical Analysis Series, Vol. 159) (Wiley, Hoboken, 2003)
2 A. Miklós, P. Hess, Z. Bozoki, Rev. Sci. Instrum. **72**, 1937 (2001)
3 A.A. Kosterev, F.K. Tittel, D.B. Serebryakov, A.L. Malinovsky, I.V. Morozov, Rev. Sci. Instrum. **76**, 043 105 (2005)
4 M.E. Webber, M. Pushkarsky, C.K.N. Patel, Appl. Opt. **42**, 2119 (2003)
5 M. Pushkarsky, M.E. Webber, C.K.N. Patel, Appl. Phys. B **78**, 673 (2003)
6 A. Schmohl, A. Miklós, P. Hess, Appl. Opt. **41**, 1815 (2002)
7 A.A. Kosterev, Y.A. Bakhirkin, R.F. Curl, F.K. Tittel, Opt. Lett. **27**, 1902 (2002)
8 J. Kauppinen, K. Wilcken, I. Kauppinen, V. Koskinen, Microchem. J. **76**, 151 (2004)
9 T. Laurila, H. Cattaneo, V. Koskinen, J. Kauppinen, R. Hernberg, Opt. Express **13**, 2453 (2005)
10 T. Laurila, H. Cattaneo, V. Koskinen, J. Kauppinen, R. Hernberg, Opt. Express **14**, 4195 (2006)
11 L.S. Rothman, D. Jacquemart, A. Barbe, D.C. Benner, M. Birk, L.R. Brown, M.R. Carleer, C. Chackerian Jr., K. Chance, L.H. Coudert, V. Dana, V.M. Devi, J.-M. Flaud, R.R. Gamache, A. Goldman, J.-M. Hartmann, K.W. Jucks, A.G. Maki, J.-Y. Mandin, S.T. Massie, J. Orphal, A. Perrin, C.P. Rinsland, M.A.H. Smith, J. Tennyson, R.N. Tolchenov, R.A. Toth, J. Vander Auwera, P. Varanasi, G. Wagner, J. Quant. Spectrosc. Radiat. Transf. **96**, 139 (2005)
12 V. Koskinen, J. Fonsen, J. Kauppinen, I. Kauppinen, Vib. Spectrosc. **42**, 239 (2006)
13 H. Cattaneo, T. Laurila, R. Hernberg, Appl. Phys. B **85**, 337 (2006)